Vol 18 No 10, October 2009
1674-1056/2009/18(10)/4242–09

Chinese Physics B

© 2009 Chin. Phys. Soc.
and IOP Publishing Ltd

Theoretical analysis of ionic autoionization spectra of lanthanum via an intermediate state [Xe]5*d*6*d* $^1P_1$*

Zhong Yin-Peng(仲银鹏), Jia Feng-Dong(贾凤东), and Zhong Zhi-Ping(钟志萍)†

Collage of Physics, Graduate University of Chinese Academy of Sciences, Beijng 100190, *China*

(Received 11 November 2008; revised manuscript received 26 May 2009)

In the framework of multi-channel quantum defect theory, eigenquantum defects μ_α and the transformation matrices $U_{i\alpha}$ of La^+ are calculated from first principles by relativistic multi-channel theory, while the dipole matrix elements D_α are obtained by fitting with experimental data. Then the ionic autoionization spectra of lanthanum via the intermediate state [Xe]5*d*6*d* $^1P_1$ in the energy region of 90213–91905 cm^{-1} are obtained. Experimental peaks are classified and assigned by comparing with the corresponding calculated spectra. More specifically, four ionic autoionization Rydberg series converging to La^{2+} $5d_{5/2}$ $^2D_{5/2}$ and several states converging to higher lying states of La^{2+} are found and assigned.

Keywords: configuration interaction, multi-channel quantum defect theory, relativistic multi-channel theory, autoionization Rydberg series

PACC: 3120T, 3150, 3280D

1. Introduction

The highly excited states of atoms and ions have been a subject of intense study, which has provided useful information for understanding electron correlation effects. Many investigations have been carried out on the highly excited states of simple atoms but fewer on those of complex atoms due to their complicated spectral structures. A lanthanum ion (La^+) with the ground state electron configuration [Xe]5d^2 can be considered as a quasi-three-body system, which can elucidate rich electron-electron correlation effects. We have measured the Rydberg and autoionization Rydberg spectra of La^+ via the intermediate state [Xe]5*d*6*d* $^1P_1$ or [Xe]5*d*6*d* $^3F_2$.[1] The energy levels of La^+ below the first ionization via the intermediate state [Xe]5*d*6*d* $^1P_1$ and [Xe]5*d*6*d* $^3F_2$, have been calculated in the framework of multi-channel quantum defect theory (MQDT)[4−10] from first principles by relativistic multi-channel theory (RMCT).[11−17] These calculations are consistent with the experimental results, thus experimental peaks are classified and clearly assigned. In Ref.[2], only the dissociation channels related to the two lowest ionization thresholds of La^+ are included. A further development is reported in Ref.[3], in which electron-electron correlation effects caused by dynamical polarizations are considered, i.e., some channels related to higher-lying ionization thresholds of La^+ are entered in the calculations. As a result, the calculations in Ref.[3] are consistent with the experimental measurement than those in Ref.[2]. With the successes of the work of Ref.[3], the ionic autoionization spectra of lanthanum via the intermediate state [Xe]5*d*6*d* $^3F_2$ in the energy region 90213–91800 cm^{-1} are calculated,[18] in which the same channels as in Ref.[3] are entered in the RMCT calculations. The calculations generally agree with the experimental spectra, and experimental peaks are classified and clearly assigned. As for the ionic autoionization spectra of lanthanum via the intermediate state [Xe]5*d*6*d* $^1P_1$, part of the ionic autoionization spectra of lanthanum, i.e., in the energy region 90650–91500 cm^{-1}, are calculated in Ref.[19], in which fewer channels are considered in the calculations than those in Refs.[3] and [18] and no assignment has been given.

The present work can be regarded as our continuing efforts on investigation of the complicated La^+ excited systems. In this paper, our interest is focused

*Project supported by the National Natural Science Foundation of China (Grant Nos 10574162 and 10774186), the Scientific Research Fund of Graduate University of the Chinese Academy of Sciences (Grant No 055101BM03).

†Corresponding author. E-mail: zpzhong@gucas.ac.cn

on the ionic autoionization spectra of lanthanum via the intermediate state [Xe]$5d6d\ ^1P_1$ in the energy region 90213–91905 cm^{-1}. Here, we adopt the same channels and same sample points of eigenquantum defects μ_α, and transformation matrices $U_{i\alpha}$ as that of Ref.[3]. Dipole matrix elements D_α are obtained by fitting with experimental spectra. With such MQDT parameters (eigenquantum defects μ_α, transformation matrices $U_{i\alpha}$ and dipole matrix elements D_α), we construct the autoionization spectra of lanthanum via the intermediate state [Xe]$5d6d\ ^1P_1$. Our calculated spectra are in general agreement with the experimental data. Based on our calculation, four autoionization Rydberg series are found and assigned as Rydberg series converging to [Xe]$5d_{5/2}\ ^2D_{5/2}$ and several broad peaks observed in experimental spectra are assigned as states converging to higher-lying states of La^{2+}.

2. Theoretical method

Within the framework of MQDT,[4−10] infinite Rydberg states and adjacent continuum states can be treated in a unified manner through a compact set of physical MQDT parameters (eigenquantum defects μ_α, transformation matrices $U_{i\alpha}$ and dipole matrix elements D_α). These MQDT parameters (eigenquantum defects μ_α, transformation matrices $U_{i\alpha}$ and dipole matrix elements D_α) are smoothly energy-dependent within the neighborhood of a threshold. This is characteristic of channel concept. They can be determined semi-empirically by fitting accurate energy levels into spectroscopic data or by the first principle calculations. However, the numerical fitting procedure requires rather complete spectroscopic data, which is always a difficult and tedious task with increasing number of related channels, thus it confines the scope of application of MQDT. In a few cases, the MQDT parameters (μ_α,$U_{i\alpha}$) can be calculated from first principles with the non-relativistic theory.[5,20] The RMCT can be regarded as an extension of the traditional configuration interaction method by including the continuum configuration interactions.[11−17] It aims directly to calculate the MQDT parameters (μ_α,$U_{i\alpha}$) and has been used to calculate atomic energy levels, Lande g factors, and the coupling scheme within the framework of MQDT.[12−17]

Since the detailed description of RMCT has been given elsewhere,[11−17] here we only give an outline. We start with a relativistic atomic Hamiltonian H, that is obtained by adopting the Coulomb gauge, namely,

$$H\psi = E\Psi \tag{1}$$

with the relativistic atomic Hamiltonian

$$\begin{aligned} H &= \sum_i^n \left(c\alpha_i \cdot P_i + \beta_i mc^2 - \frac{Ze^2}{r_i} \right) + \sum_{i>j} \frac{e^2}{r_{ij}} \\ &= H_0 + V. \end{aligned} \tag{2}$$

Here H_0 is a relativistic self-consistent field (SCF) atomic Hamiltonian and V is a residual interaction. The Breit interactions and the rest of the higher-order quantum electrodynamical interactions are not included and can be treated as perturbations later.

From such a complete set of single-electron wave functions, i.e., orbital, bound and continuum configuration wave functions (Φ_n and $\Phi_{j\epsilon}$) are constructed the anti-symmetrized product-type wave functions of N single-electron wave functions with certain electron occupation distributions and appropriate angular momentum couplings. Such configuration functions form bases of the complete Hilbert space for the atomic system with N electrons. Wave functions of energy eigenstates can be expressed as,[11−17]

$$\Psi(E,i) = \sum_n A_n(E,i)\phi_n + \sum_j \int_{\epsilon_c} B_{j\epsilon}(E,i)\Phi_{j\epsilon} \mathrm{d}\epsilon. \tag{3}$$

The index j refers to various dissociation channels. The coefficients of linear superposition, $A_n(E,i)$ and $B_{j\epsilon}(E,i)$, can be expressed in terms of K matrix,

$$A_n(E,i) = \frac{K_{n,iE}}{E - E_n^0} \cdot N(E,i), \tag{4}$$

$$B_{j\epsilon}(E,i) = \left[\mathrm{P}\frac{K_{j\epsilon,iE}}{E-\epsilon} + \delta_{ji} \cdot \delta(\epsilon - E) \right] \cdot N(E,i). \tag{5}$$

Here, P represents principal integration, $N(E,i)$ is the nomalization factors. With the calculated matrix elements of residual interactions $V_{n,n'}$, $V_{n,j\epsilon}$, $V_{j\epsilon,j'\epsilon'}$ (representing discrete–discrete, discrete–continuum, continuum–continuum interactions respectively), it then leads to Lippmann–Schwinger integral equations of the K matrix at $E \geq \epsilon_c$,

$$K_{n',iE} = V_{n',iE} + \sum_j \int_{\epsilon_c} \frac{V_{n',j\epsilon} K_{j\epsilon,iE}}{E-\epsilon} \mathrm{d}\epsilon$$

$$+\sum_n \frac{V_{n',n}K_{n,iE}}{E-E_n^0}, \tag{6}$$

$$K_{j'\epsilon',iE} = V_{j'\epsilon',iE} + \sum_j \int_{\epsilon_c} \frac{V_{j'\epsilon',j\epsilon}K_{j\epsilon,iE}}{E-\epsilon}\mathrm{d}\epsilon + \sum_n \frac{V_{j'\epsilon',n}K_{n,iE}}{E-E_n^0}. \tag{7}$$

Here E_n^0, ϵ are the eigenvalues of H_0 corresponding to the eigenfunctions Φ_n and $\Phi_{j,\epsilon}$, respectively. After solving the integral equation, the physical parameters (eigenquantum defects μ_α and transformation matrix $U_{i\alpha}$) in MQDT can be obtained directly by diagonalizing the K matrix on the energy shell.[11−17] In the autoionization region, μ_α and $U_{i\alpha}$ are related as,

$$\begin{aligned} &\mathrm{Det}|F_{i\alpha}| \\ &= \mathrm{Det}|U_{i\alpha}\sin[\pi(x_i+\mu_\alpha)]| \\ &= 0 \begin{cases} x_i = \nu_i & i \in \bar{Q}, \\ x_i = -\tau_\rho & i \in \bar{P}. \end{cases} \end{aligned} \tag{8}$$

For the closed dissociation channels ($i \in \bar{Q}$), ν_i is the effective quantum number of the i-th channel. Each collision eigenstate ρ is a superposition of the standing waves of open dissociation channels ($i \in \bar{P}$) with the same eigenphase shift $\pi\rho$. The reduced dipole matrix element from the initial state to the ρ-th autoionization eigenchannel can be written as[10]

$$\mathcal{D}_\rho = \sum_\alpha D_\alpha A_\alpha^\rho + D_{cc,\rho}, \tag{9}$$

where D_α is the dipole matrix element for the channel excitation and $D_{cc,\rho}$ is the matrix element for core excitation. The mixing coefficient A_α^ρ is determined as

$$A_\alpha^{(\rho)} = B_\alpha^{(\rho)}/N_\rho, \tag{10}$$

$$B_\alpha^{(\rho)} = C_{j\alpha}(\{\nu_i; i \in \bar{Q}\}, \tau_\rho) \cdot \left\{\sum_\alpha [C_{j\alpha}(\{\nu_i; i \in \bar{Q}\}, \tau_\rho)]^2\right\}^{1/2}, \tag{11}$$

$$N_\rho^2 = \sum_{i\in\bar{Q}} \left[\sum_\alpha U_{i\alpha}\cos\pi(\tau_\rho+\mu_\alpha)B_\alpha^{(\rho)}\right], \tag{12}$$

where the index j can be chosen arbitrarily, and the $C_{j\alpha}(\{\nu_i; i \in \bar{Q}\}$ is the cofactor of the element of the j-th row and α-th column of the determinant $|F_{j\alpha}|$ in Eq.(8).

For a particle with charge Z, the excitation energy E in the autoionization region can be expressed in terms of quantum defect μ or effective quantum number n^*:

$$E = I_i - \frac{(Z+1)^2}{2(n-\mu)^2} = I_i - \frac{(Z+1)^2}{2n^{*2}}, \tag{13}$$

where I_i represents the i-th autoionization threshold. With a specified energy E which lies in continua energy levels, we can obtain the corresponding n^* for the i-th dissociation channel from Eq.(13).

In the energy region of interest, the spectra are far away from the core excitation, thus

$$\mathcal{D}_\rho \sim \sum_\alpha D_\alpha A_\alpha^\rho. \tag{14}$$

Then the scattering cross sections are,[4,5,7,9,10]

$$\begin{aligned} \sigma &= 2\pi^2\alpha a_0^2(\mathrm{d}f/\mathrm{d}\epsilon) \\ &= 4\pi^2\alpha a_0^2\omega\sum_\rho D_\rho^2 \\ &= \sum_\rho \left(\sum_\alpha D_\alpha A_\alpha^\rho\right)^2, \end{aligned} \tag{15}$$

where $(\mathrm{d}f/\mathrm{d}\epsilon)$ is the density of oscillator strengths, α is the fine structure constant, $a_0 = 0.529$ Å (1 Å = 0.1 nm), ω is the photon energy in atomic units (a.u.).

Because of the smoothness of a channel, we only calculate MQDT parameters at a few energy points across the threshold, then these MQDT parameters at any energy point within the neighborhood of threshold can be obtained by interpolating or extrapolating from the calculated data. In fact, eigenquantum defects μ_α, transformation matrices $U_{i\alpha}$ in this paper and those in Ref.[3] are obtained by extrapolating from the same calculated data. As for the dipole matrix elements D_α, they can be assumed as constants within the energy region of interest.

As for the assignment of an autoionization state, according to Eq.(15), the spectra of the autoionization states can be obtained from the mixing of different autoionization eigenchannels ρ and then different eigenchannels α. Usually, if one specific peak in the experimental spectra mainly comes from one eigenchannel, the peak can be assigned as an autoionization state belonging to this eigenchannel. Similar to the work of Ref.[18], we do the assignment as follows: first we calculate the eigenchannel spectra for a specific eigenchannel α by setting $D_{\alpha'} = \delta_{\alpha\alpha'}$. Then compare this eigenchannel spectra with the experimental ones in terms of energy position to assign specific peaks. Clearly, this eigenchannel spectra may not correctly reflect the profile for a specific peak, especially

for the strongly perturbed resonance, when the interaction between bound and continuum states is strong, which forms the Fano profile,[21] but it can meet the purpose of assignment in normal cases. As for the energy position of an autoionization state, it can be determined by fitting Fano profile[21] in the simplest case, i.e., just two channels are considered or by fitting Shore's parametrization[22] in a complicated case. However, since there are more than 10 channels in this work, here we simply determine the resonance energy position of an autoionization state by its maximum. In addition, since the energy resolution in the experimental spectra is about 0.5 cm^{-1}, we convolute theoretical spectra with a Gaussian profile of 0.5 cm^{-1} full width of half maximum.

3. Results and discussion

The experimental autoionization spectra of La^+ via the intermediate states $5d6d\ ^1P_1$ in the energy region 90213–91905 cm^{-1} are shown in Fig.1. Clearly, there are two distinct ionic autoionization Rydberg series and some strong broad peaks (labeled as A, B, C, D and E, shown in Fig.1). We will first analyze these ionic autoionization Rydberg series, and then the broad peaks one by one.

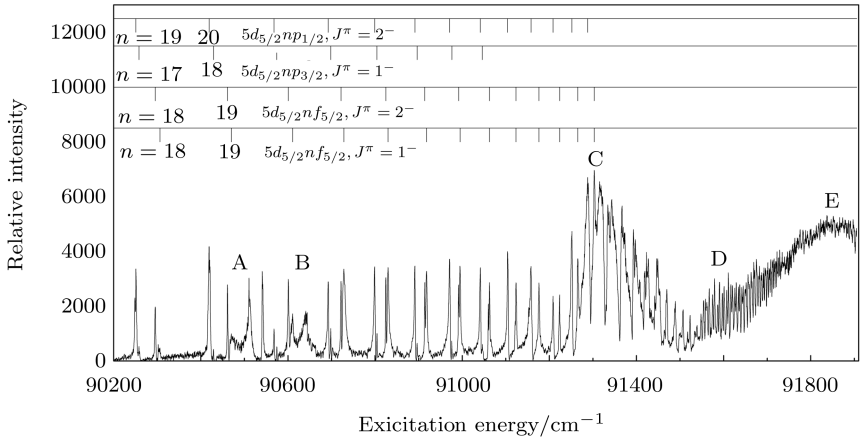


Fig.1. The experimental spectra of La^+ via the intermediate state [Xe]$5d6d\ ^1P_1$ in the energy region 90200–91800 cm^{-1}.[1] Four ionic autoionization Rydberg series were assigned.

First, we discuss these ionic autoionization Rydberg series, with energy positions shown in Tables 1-4. as well as the effective quantum numbers n^* obtained by Eq.(13). Clearly, there are four ionic autoionization Rydberg series converging to [Xe]$5d_{(5/2)}\ 2D_{5/2}$. More specifically, two distinct ionic autoionization Rydberg series mentioned above and two weak ionic autoionization Rydberg series. Note that peaks above 91303 cm^{-1} are missing in Tables 1-4; the reason for this can be attributed to the configuration interaction among these Rydberg states and neighbouring states converging to higher-lying states of La^{2+}. It results in a rapid change of shape and energy position for a specific state as shown in Fig.1. Such a strong wavefunction mixing makes the assignment meaningless. Figure 2 shows some calculated eigenchannel spectra related to the autoionization Rydberg series converging to [Xe]$5d_{(5/2)}\ 2D_{5/2}$. Through comparison with the experimental spectra via the intermediate state [Xe]$5d6d\ ^1P_1$, the two distinct ionic autoionization Rydberg series are assigned as $5d_{5/2}np_{1/2}\ J^\pi = 2^-$ and $5d_{5/2}nf_{5/2}\ J^\pi = 2^-$, respectively, and the two weak ionic autoionization Rydberg series are assigned as $5d_{5/2}np_{3/2}\ J^\pi = 1^-$ and $5d_{5/2}nf_{5/2}\ J^\pi = 1^-$, respectively. As shown in Tables 1–4, the difference between experimental and calculated quantum defects, i.e., $\Delta\mu$, is generally in the range of 0.01–0.15 for $n^* \leq 24$, and $\Delta\mu$ is in the range of 0.15–0.30 for $n^* > 24$. The fact that $\Delta\mu$ becomes larger as n increases is due to $\Delta\mu = \Delta E n^{*3}$ based on Eq.(13). Here ΔE is the difference between experimental and calculated energy levels. Therefore, the error in the quantum defect in-

creases rapidly as n gets larger even if there is a small error in energy level. On the other hand, it is reasonable to deduce that some low n states belonging to these autoionization Rydberg series should be observed in the experimental spectra below the first ionization threshold. In fact, Zhang *et al*[3] have observed some states converging to $5d_{5/2}\ ^2D_{5/2}$, and assigned them as $5d_{5/2}np_{1/2}\ J^\pi = 2^-$, $5d_{5/2}nf_{5/2}\ J^\pi = 2^-$ and $5d_{5/2}nf_{5/2}\ J^\pi = 1^-$. The reason why these states belonging to $5d_{5/2}np_{3/2}\ J^\pi = 1^-$ have not observed in Ref.[3] may be due to the fact that it is too weak to be observed. Therefore, the assignments in the present work is consistent with those of Ref.[3].

Table 1. Comparison of energy positions (cm^{-1}) between the present calculated and experimental autoionization Rydberg series $5d_{5/2}np_{1/2}\ J^\pi = 2^-$.

$E_{exp.}$	$n^*_{exp.}$	$E_{theor.}$	$\Delta\mu = \mu_{exp.} - \mu_{theor.}$
90251.1	16.74	90239.1	0.06
90419.0	17.73	90412.4	0.05
90568.0	18.75	90559.1	0.06
90692.4	19.76	90682.4	0.08
90799.1	20.78	90787.9	0.12
90891.4	21.79	90882.7	0.10
90970.9	22.79	90963.0	0.11
91041.6	23.81	91033.0	0.13
91104.2	24.83	91090.5	0.23
91157.8	25.82	91150.9	0.13
91208.4	26.88	91199.2	0.20
91251.8	27.89	91242.2	0.23
91288.5	28.85	91281.3	0.20

Table 2. Comparison of energy positions (cm^{-1}) between the present calculated and experimental autoionization Rydberg series $5d_{5/2}nf_{5/2}\ J^\pi = 2^-$.

$E_{exp.}$	$n^*_{exp.}$	$E_{theor.}$	$\Delta\mu = \mu_{exp.} - \mu_{theor.}$
90295.4	17.00	90297.6	0.00
90461.2	18.00	90459.5	0.01
90600.8	19.00	90599.4	0.01
90722.0	20.03	90717.2	0.04
90824.9	21.04	90818.9	0.06
90914.1	22.06	90907.9	0.07
90991.8	23.08	90984.3	0.11
91060.0	24.10	91052.5	0.12
91121.2	25.13	91113.1	0.14
91176.3	26.19	91165.5	0.21
91223.7	27.22	91213.2	0.24
91265.2	28.23	91254.6	0.27
91303.0	29.25	91292.5	0.29

Now we focus on these broad peaks A, B, C, D and E. These peaks should correspond to autoionization states converging to higher-lying states of La^{2+}. Such broad profiles may be due to strong interactions with neighbouring autoionization Rydberg series. First, we analyse the broad peak A located around 90500 cm^{-1}. Figure 3(a) shows the calculated spectra for eigenchannel $4f_{7/2}nd_{5/2}\ J^\pi = 1^-$. Clearly, there is a broad peak located around 90380 cm^{-1} and is close to peak A. Therefore, peak A may be related to channel $4f_{7/2}nd_{5/2}\ J^\pi = 1^-$; furthermore, the broad peak A may be mainly assigned as $4f_{7/2}10d_{5/2}\ J^\pi = 1^-$ ($n^* = 7.23$). The principal quantum number is deduced from the experimental energy level $4f5d\ J^\pi = 1^-$ (energy level = 21441.73 cm^{-1}, $n^* = 2.38$).[23] Small peaks in other energy regions of Fig.3(a) come from configuration interaction with other channels of Rydberg series converging to $5d_{5/2}\ ^2D_{5/2}$.

Table 3. Comparison of energy positions (cm^{-1}) between the present calculated and experimental autoionization Rydberg series $5d_{5/2}nf_{5/2}\ J^\pi = 1^-$.

$E_{exp.}$	$n^*_{exp.}$	$E_{theor.}$	$\Delta\mu = \mu_{exp.} - \mu_{theor.}$
90306.1	17.05	90298.4	0.04
90470.1	18.06	90461.8	0.06
90610.1	19.08	90601.4	0.09
90728.2	20.09	90718.6	0.03
90830.0	21.10	90819.8	0.01
90918.1	22.11	90908.6	–0.02
90995.0	23.12	90986.8	–0.03
91062.6	24.13	91054.6	–0.06
91123.5	25.18	91114.0	–0.07
91176.3	26.19	91166.2	–0.2
91223.7	27.22	91212.3	–0.26
91265.2	28.23	91253.9	–0.29
91303.0	29.25	91291.6	–0.32

Table 4. Comparison of energy positions (cm^{-1}) between the present calculated and experimental autoionization Rydberg series $5d_{5/2}np_{3/2}\ J^\pi = 1^-$.

$E_{exp.}$	$n^*_{exp.}$	$E_{theor.}$	$\Delta\mu = \mu_{exp.} - \mu_{theor.}$
90257.9	16.78	90243.5	0.07
90429.3	17.79	90413.0	0.10
90574.5	18.80	90557.2	0.13
90698.3	19.82	90679.6	0.17
90804.2	20.83	90785.5	0.19
90896.5	21.85	90876.9	0.23
90976.1	22.86	90956.6	0.26
91046.2	23.88	91026.6	0.30

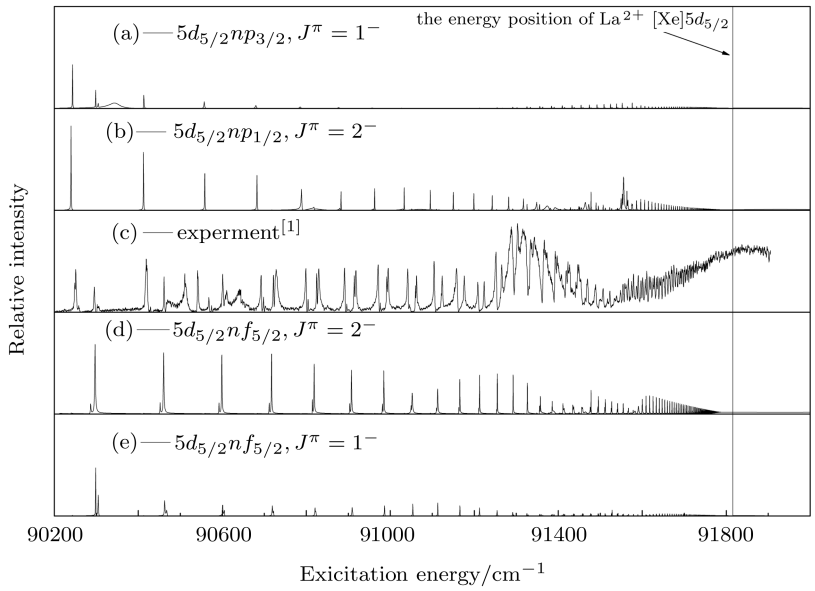


Fig.2. Comparison of the present calculated eigenchannel spectra related to ionic autoionization Rydberg converging to [Xe]$5d_{(5/2)}$ $2D_{5/2}$ with the experimental spectra[1] of La^+ via the intermediate state [Xe]$5d6d\ ^1P_1$. (a) The calculated autoionization spectra for eigenchannel $5d_{5/2}np_{3/2}, J^\pi = 1^-$; (b) the calculated autoionization spectra for eigenchannel $5d_{5/2}np_{1/2}, J^\pi = 2^-$; (c) the experimental spectra; (d) the calculated autoionization spectra for eigenchannel $5d_{5/2}nf_{5/2}, J^\pi = 2^-$; (e) the calculated autoionization spectra for eigenchannel $5d_{5/2}nf_{5/2}, J^\pi = 1^-$.

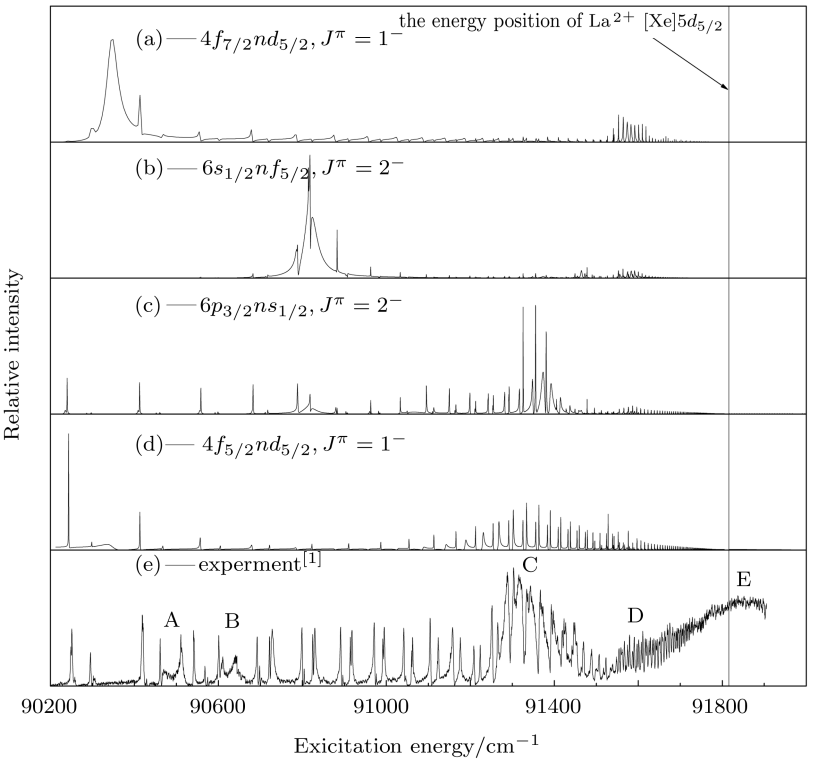


Fig.3. Comparison of the present calculated eigenchannel spectra related to broad peaks A, B, C with the experimental spectra[1] of La^+ via the intermediate state [Xe]$5d6d\ ^1P_1$. (a) The calculated autoionization spectra for eigenchannel $4f_{7/2}nd_{5/2}, J^\pi = 1^-$; (b) the calculated autoionization spectra for eigenchannel $6s_{1/2}nf_{5/2}, J^\pi = 2^-$; (c) the calculated autoionization spectra for eigenchannel $6p_{3/2}ns_{1/2}, J^\pi = 2^-$; (d) the calculated autoionization spectra for eigenchannel $4f_{5/2}nd_{5/2}, J^\pi = 1^-$; (e) the experimental spectra.

Second, we discuss the broad peak B located around 90627 cm^{-1}. Figure 3(b) shows the calculated spectra for eigenchannel $6s_{1/2}nf_{5/2}$ $J^{\pi} = 2^{-}$. There is a broad peak located around 90850 cm^{-1}, so it may be related to channel $6s_{1/2}$ (7 or 8) $f_{5/2}$ $J^{\pi} = 2^{-}$, $n^{*} = 5.77$. The principal quantum number is deduced from the experimental energy level $4f(2F^{0}_{5/2})6s_{1/2}$ $J^{\pi} = 2^{-}$ (energy level = 14147.98 cm^{-1}, $n^{*} = 2.21$).[23]

Next, we discuss the broad peak C located around 91300 cm^{-1} shown in Fig.3(e). Note that some peaks embedded in this energy region are closely spaced in energy, these states should be related to the ionic autoionization Rydberg series converging to [Xe]$5d_{(5/2)}$ $2D_{5/2}$, such ionic autoionization Rydberg states may strongly interact with an autoionization state converging to higher-lying states of La^{2+}, which results in a rapid change in shape and energy position for the autoionization states and these ionic autoionization Rydberg states as shown in Fig.3(e). Figure 3(c) shows the calculated autoionization spectra for eigenchannel $6p_{3/2}ns_{1/2}$ $J^{\pi} = 2^{-}$ and figure 3(d) shows the calculated autoionization spectra for eigenchannel $4f_{5/2}nd_{5/2}$ $J^{\pi} = 1^{-}$. In both of the two eigenchannel spectra, there are some broad peaks closely spaced in energy region around 91300 cm^{-1}, which are similar to peak C in Fig.3(e). So broad peak C may be related to eigenchannels $4f_{5/2}nd_{5/2}$ $J^{\pi} = 1^{-}$ and/or $6p_{3/2}ns_{1/2}$ $J^{\pi} = 2^{-}$. They may be assigned as $4f_{5/2}11d_{5/2}$ ($n^{*} = 8.48$) $J^{\pi} = 1^{-}$ and/or $6p_{3/2}$(9 or 10)$s_{1/2}$ ($n^{*} = 5.92$) $J^{\pi} = 2^{-}$. The principal quantum number is deduced from the experimental energy levels $4f5d$ $J^{\pi} = 1^{-}$ (energy level = 21441.73 cm^{-1}, $n^{*} = 2.40$)[23] and $6s6p$ $J^{\pi} = 2^{-}$ (energy = 29498.05^{-1}, $n^{*} = 2.43$).[23] Furthermore, there are some ionic autoionization Rydberg series emerging in both of the two eigenchannel spectra, which come from configuration interaction among autoionization states converging to $4f_{5/2}$ and/or $6p_{3/2}$ and ionic auto-Rydberg series converging to $5d_{5/2}$ $^{2}D_{5/2}$.

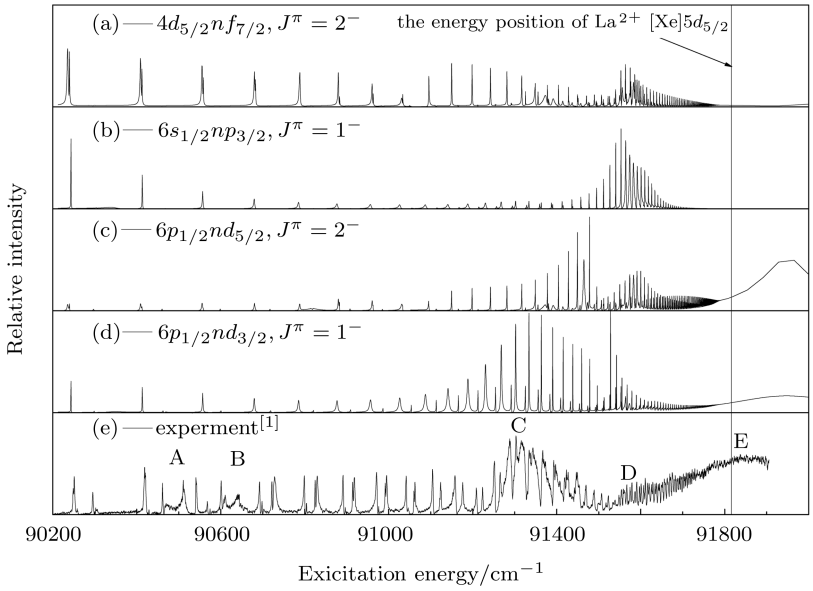


Fig.4. Comparison of the present calculated eigenchannel spectra related to broad peaks D, E with the experimental spectra[1] of La^{+} via the intermediate state [Xe]$5d6d$ $^{1}P_{1}$. (a) The calculated autoionization spectra for eigenchannel $4d_{5/2}nf_{7/2}, J^{\pi} = 2^{-}$; (b) the calculated autoionization spectra for eigenchannel $6s_{1/2}np_{3/2}, J^{\pi} = 1^{-}$; (c) the calculated autoionization spectra for eigenchannel $6p_{1/2}nd_{5/2}, J^{\pi} = 2^{-}$; (d) the calculated autoionization spectra for eigenchannel $6p_{1/2}nd_{3/2}, J^{\pi} = 1^{-}$; (e) the experimental spectra.

Now we discuss the peak D located around 91584 cm^{-1}, which is weak and broad. Similar to the peak C, many peaks closely spaced in energy are embedded in the peak D; these states should be related to the ionic autoionization Rydberg series converging to [Xe]$5d_{(5/2)}$ $2D_{5/2}$. Figure 4(a) shows the calculated autoionization spectra for eigenchannel $4f_{7/2}nd_{5/2}$ $J^{\pi} = 2^{-}$, and figure 4(b) shows the calculated autoionization spectra for eigenchannel $6s_{1/2}np_{3/2}$ $J^{\pi} = 1^{-}$, both of them have broad peak around 91584 cm^{-1}. Therefore, the

broad peak D may be related to eigenchannels $6s_{1/2}np_{3/2}$ $J^\pi = 1^-$ and/or $4f_{7/2}nd_{5/2}$ $J^\pi = 2^-$. They may be assigned as $6s_{1/2}$ (9 or 10) $p_{3/2}$ $J^\pi = 1^-$ ($n^* = 5.99$) and/or $4f_{7/2}$ (10 or 11) $d_{5/2}$ $J^\pi = 2^-$ ($n^* = 7.74$). The principal quantum numbers are deduced from experimental level $6s6p$ $J^\pi = 1^-$, (energy level = 28154.55 cm^{-1}, $n^* = 2.41$),[23] and $4f5d$ $J^\pi = 2^-$, (energy level = 17211.93 cm^{-1} $n^* = 2.32$).[23] Similarly, there are some ionic autoionization Rydberg series emerging in both of the two eigenchannel spectra, which come from configuration interaction between autoionization state converging to $6s_{1/2}$ and/or $6d_{5/2}$ and ionic auto-Rydberg series converging to $5d_{5/2}$ $^2D_{5/2}$.

Finally, we discuss the peak E located around 91852 cm^{-1}. Figure 4(c) shows the calculated autoionization spectra for eigenchannel $6p_{1/2}nd_{5/2}$ $J^\pi = 2^-$, and figure 4(d) shows the calculated autoionization spectra for eigenchannel $6p_{1/2}nd_{3/2}$ $J^\pi = 1^-$. In both of the two eigenchannel spectra, there is a broad peak close to 91852 cm^{-1}, so the broad peak E may be related to eigenchannels $6p_{1/2}nd_{3/2}$ $J^\pi = 1^-$ and/or $6p_{1/2}nd_{5/2}$ $J^\pi = 2^-$. Similarly, it may be assigned as $6p_{1/2}$ (6 or 7) $d_{3/2}$ ($n^* = 3.30$) $J^\pi = 1^-$ and/or $6p_{1/2}$ (6 or 7) $d_{5/2}$ ($n^* = 3.30$) $J^\pi = 2^-$. The principal quantum numbers are deduced from experimental level of $5d6p$ $J^\pi = 1^-$ (energy level = 25973.37 cm^{-1}, $n^* = 2.03$)[23] and experimental level of $5d6p$ $J^\pi = 2^-$ (energy level = 24462.66 cm^{-1}, $n^* = 2.02$).[23] There are some ionic autoionization Rydberg series emerging in both of the two eigenchannel spectra, which come from configuration interaction between autoionization state converging to $6p_{1/2}$ and ionic autoionization Rydberg series converging to $5d_{5/2}$ $^2D_{5/2}$.

Table 5 gives the summary for the assignments for the broad peaks A, B, C, D and E. Clearly, the calculated energy positions for these peaks agree well with the experimental data. In fact, the difference between experimental and calculated quantum defects is in the range of 0–0.07.

Table 5. Comparison of energy positions (cm^{-1}) between the present calculated and experimental autoionization states converging to higher-lying states of La^{2+}. The assignment is indicated in the parentheses.

peak	$E_{\text{exp.}}$	$E_{\text{theor.}}$			
		$J^\pi = 1^-$	$\Delta\mu$	$J^\pi = 2^-$	$\Delta\mu = \mu_{\text{exp.}} - \mu_{\text{theor.}}$
A	∼90500	∼90380	0.05		
		($4f_{7/2}10d_{5/2}$)			
B	∼90627			∼90850	0.05
				($6s_{1/2}$ (7 or 8) $f_{5/2}$)	
C	∼91300	∼91380	–0.07	∼91380	0.00
		($4f_{5/2}11d_{5/2}$)		($6p_{3/2}$ (9 or 10) $s_{1/2}$)	
D	∼91584	∼91584	0.00	∼91584	0.00
		($6s_{1/2}$(9 or 10)$p_{3/2}$)		($4f_{7/2}$ (10 or 11) $f_{5/2}$)	
E	∼91852	∼91934	0.00	∼91934	0.00
		($6p_{1/2}$ (6 or 7) $d_{3/2}$)		($6p_{1/2}$ (6 or 7) $d_{5/2}$)	

Based on the above work, we have determined the eigenchannels that give primary contribution to the peaks observed in ionic autoionization experimental spectra of lanthanum via the intermediate state [Xe]$5d6d$ $^1P_1$. By adjusting D_α, which is shown in Table 6, we reconstruct the autoionization spectra of La^+ via the intermediate state [Xe]$5d6d$ $^1P_1$ shown in Fig.5. Note that there are discrepancies between the present calculated spectra and the experimental spectra in some energy regions in intensities and positions, such as in the energy regions around 91300 cm^{-1} and 91600 cm $^{-1}$. This may be due to the procedure of selecting primary eigenchannels. The omitted eigenchannels may affect the profile in certain energy regions. But the present work should meet the purpose of assignment in most cases.

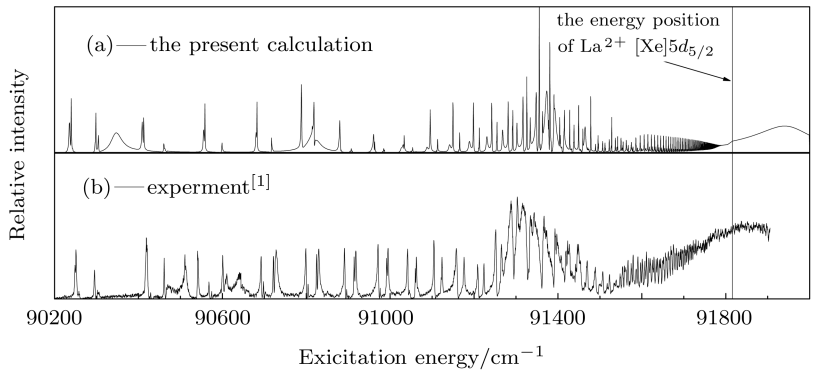


Fig.5. Comparison of the present calculated spectra (a) with the experimental spectra (b) of La^+ via the intermediate state [Xe]5d6d $^1P_1$. Only eigenchannels with the non-trivial D_α listed in Table 5 are included.

Table 6. Eigenchannels included in constructing the calculated spectra and the corresponding dipole matrix elements D_α of the eigenchannels. D_α is obtained by fitting with the experimental spectra.

$J^\pi = 1^-$		$J^\pi = 2^-$	
channels	D_α	channels	D_α
$5d_{5/2}\epsilon f_{5/2}$	0.8	$5d_{5/2}\epsilon f_{5/2}$	–1.0
$5d_{5/2}\epsilon p_{1/2}$	–0.3	$5d_{5/2}\epsilon p_{1/2}$	0.5
$4f_{7/2}\epsilon d_{5/2}$	–0.5	$6s_{1/2}\epsilon f_{5/2}$	–3.0
$4f_{5/2}\epsilon d_{5/2}$	–4.0	$6p_{3/2}\epsilon s_{1/2}$	1.0
$6s_{1/2}\epsilon p_{3/2}$	0.1	$4d_{5/2}\epsilon f_{7/2}$	–6.0
$6p_{1/2}\epsilon d_{3/2}$	4.0	$6p_{1/2}\epsilon d_{5/2}$	25.0

4. Conclusion

In summary, in the framework of the multichannel quantum defect theory, eigenquantum defects μ_α and transformation matrices $U_{i\alpha}$ of La^+ are calculated from first principles by using relativistic multichannel theory; while the dipole matrix elements D_α are obtained by fitting experimental data shown in Table 6. With these MQDT parameters, we reconstruct the autoionization spectra of La^+ via the intermediate state [Xe]5d6d $^1P_1$. As shown in Fig.5, our calculated spectra generally agree well with the experimental spectra.[1] Based on our calculations, four ionic autoionization Rydberg series are found and assigned as $5d_{5/2}np_{1/2}$ $J^\pi = 2^-$, $5d_{5/2}nf_{5/2}$ $J^\pi = 2^-$, $5d_{5/2}nf_{5/2}$ $J^\pi = 1^-$ and $5d_{5/2}np_{3/2}$ $J^\pi = 1^-$, respectively, as shown in Figs.1 and 2, Tables 1-4. There are also several broad peaks observed in the experimental spectra to be assigned as states converging to higher levels of La^{2+}, as shown in Figs.3 and 4, and Table 5.

References

[1] Xie X P, Xu C B, Sun W, Xue P, Zhong Z P, Huang W and Xu X Y 1999 *J. Opt. Soc. Am.* B **16** 484
[2] Sun W, Yan J, Zhong Z P, Xie X P, Xue P and Xu X Y 2001 *J. Phys.* B: *At. Mol. Opt. Phys.* **34** 369
[3] Zhang X F, Jia F D, Zhong Z P, Xue P, Xu X Y and Yan J 2007 *Chin. Phys. Lett.* **24** 2808
[4] Lee C M (Li J M) and Johnson W R 1980 *Phys. Rev.* A **22** 979
[5] Lee C M (Li J M) and Lu K T 1973 *Phys. Rev.* A **8** 1241
[6] Fano U 1970 *Phys. Rev.* A **2** 353
[7] Seaton M J 1983 *Rep. Prog. Phys.* **46** 167
[8] Greene C, Fano U and Strinati G 1979 *Phys. Rev.* A **19** 1485
[9] Li J M 1980 *Acta Phys. Sin.* **29** 419 (in Chinese)
[10] Li J M 1983 *Acta Phys. Sin.* **32** 84 (in Chinese)
[11] Zou Y, Tong X M and Li J M 1995 *Acta Phys. Sin.* **44** 50 (in Chinese)
[12] Huang W, Zou Y, Tong X M and Li J M 1995 *Phys. Rev.* A **52** 2770
[13] Li J M, Wu Y J and Pratt R H 1989 *Phys. Rev.* A **40** 3036
[14] Yan J, Zhang P H, Tong X M and Li J M 1996 *Acta Phys. Sin.* **45** 1978 (in Chinese)
[15] Xia D and Li J M 2001 *Chin. Phys. Lett.* **18** 1334
[16] Xia D, Zhang S Z, Peng Y L and Li J M 2003 *Chin. Phys. Lett.* **20** 56
[17] Lee C M (Li J M) 1974 *Phys. Rev.* A **10** 584
[18] Wang J Y, Zhong Z P, Jia F D, Qu Y Z and Zhong Y P 2008 *J. Phys.* B: *At. Mol. Opt. Phys.* **41** 085002
[19] Zhang X F, Peng Y L, Zhong Z P, Qu Y Z, Sun W, Xia D, Xue P and Xu X Y 2003 *Chin. Phys. Lett.* **20** 1242
[20] Aymar M 1984 *Phys. Rep.* **110** 163
[21] Fano U 1961 *Phys. Rev.* **124** 1866
[22] Shore B W 1968 *Phys. Rev.* **171** 43
[23] Sansonetti J E and Martin W C 2005 *J. Phys. Chem. Ref. Data* **34** 1559